American Mineralogist, Volume 76, pages 1701–1707, 1991

Ashburtonite, a new bicarbonate-silicate mineral from Ashburton Downs, Western Australia: Description and structure determination

Joel D. Grice
Mineral Sciences Section, Canadian Museum of Nature, Ottawa, Ontario K1P 6P4, Canada
Ernest H. Nickel
Division of Mineral Products, CSIRO, Wembley, Western Australia 6014, Australia
Robert A. Gault
Mineral Sciences Section, Canadian Museum of Nature, Ottawa, Ontario K1P 6P4, Canada

Abstract

Ashburtonite, ideally $HPb_4Cu_4Si_4O_{12}(HCO_3)_4(OH)_4Cl$, is a new mineral from Ashburton Downs, Western Australia. It occurs as clusters of clear blue, prismatic crystals up to 0.4 mm long. Associated minerals include diaboleite, duftite, beudantite, caledonite, plattnerite, cerussite, malachite, and brochantite. The mineral has a vitreous luster and light blue streak. It is brittle with a conchoidal fracture. Ashburtonite is uniaxial positive with $\omega = 1.786(3)$ and $\epsilon = 1.800(4)$. It is tetragonal, space group $I4/m$, with $a = 14.234(7)$, $c = 6.103(5)$ Å, and $Z = 2$. The strongest X-ray powder-diffraction lines are [d (Å), I, hkl] 10.2(100,110), 5.644(70,101), 4.495(100,310), 3.333(100,321), 3.013(90,411), 2.805(30,202), 2.611(50,222), 2.010(30,710,103,631), 1.656(30,642,503). Crystals are elongated on [001] with forms {110}, {100}, {001}, and {301}. The infrared spectrum indicates the presence of OH and CO_3 groups. An electron-microprobe analysis gave PbO 52.2, CuO 18.7, SiO_2 14.1, Cl 2.3, H_2O(calc.) 4.22 and CO_2(calc.) 10.31, $-O \equiv Cl = 0.51$, total 101.20 wt%; $D_{calc} = 4.69$ g/cm^3. The structure has been refined to $R = 3.5$ and $R_w = 2.4\%$. The four-membered, tetrahedral silicate rings are cross linked by ribbons of edge-shared Cu octahedra. The [HCO_3] groups are loosely bonded to the sides of large c axis channels by Cu octahedra and Pb in ninefold coordination. The Pb^{2+} has a stereochemically inactive lone pair of electrons, which causes a lowering of symmetry in the atomic structure.

Introduction

There are many small copper deposits in the Capricorn Range approximately 1000 km north of Perth, Western Australia. The new mineral, ashburtonite, was found at the Anticline prospect, on Mineral Claim 84, which is on the Ashburton Downs pastoral lease, 11.2 km west-southwest of Ashburton Downs homestead. The specimens used in the present description were collected by Blair Gartrell and brought to E.H.N. Gartrell had noted several rare species and a number of unusual minerals that he could not identify. His astute observations have now resulted in the description of two new mineral species: gartrellite (Nickel et al., 1989), named in his honor, and ashburtonite, described in the present paper.

The new mineral and the name were approved by the Commission on New Minerals and Mineral Names, IMA. Cotype material is in the Collection of the Canadian Museum of Nature under catalog no. CMN 58391 and in the Museum of Victoria, Melbourne, under catalog no. M40712.

Occurrence

The Anticline prospect at Ashburton Downs has an assemblage of secondary minerals in a weathered shear zone that cuts a series of shales and graywackes. The secondary minerals were probably derived from a primary sulfide assemblage including chalcopyrite and galena, but they are not available for study. However, a few residual relic galena crystals can be observed in the secondary assemblage. The secondary assemblage consists essentially of hydrated carbonates, arsenates and sulfates of Pb and Cu, and to a much lesser extent, Zn and Fe. Associated with the new mineral ashburtonite are beudantite, brochantite, caledonite, cerussite, diaboleite, duftite, malachite, and plattnerite. Nickel et al. (1989) also report the presence of adamite, antlerite, bayldonite, bindheimite, carminite, chenevixite, chlorargyrite, chrysocolla, cinnabar, coronadite, cumengite, gartrellite, goethite, hematite, hemimorphite, hydrozincite, jarosite, lavendulan, linarite, mimetite, olivenite, paratacamite, and rosasite at this locality.

0003–004X/91/0910–1701$02.00

Fig. 1. Scanning electron microscope photomicrograph showing ashburtonite crystals elongated on [001]. Scale bar is 10 μm.

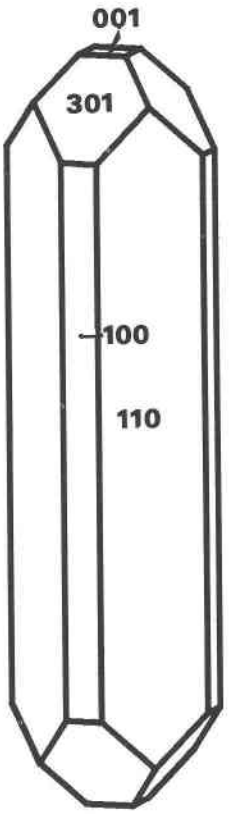

Fig. 2. Crystal drawing of ashburtonite, clinographic projection.

Physical, optical, and chemical properties

Ashburtonite occurs as very small crystals, distinctly blue with no greenish tint, up to 400 μm long and 30 μm wide clustered in aggregates up to 20 mm in diameter (Fig. 1). Ashburtonite crystals are prismatic, elongated parallel to [001] with a dominant prism {110} and sometimes a minor prism {100}, and terminated by a pinacoid {001} or a combination of a pinacoid and pyramid {301} faces (Fig. 2). A dipyramidal development was noted on some crystals.

Ashburtonite is transparent, with a vitreous luster and pale blue streak. Crystals are very brittle, breaking with a conchoidal fracture and no apparent cleavage. Hardness could not be determined because of the small grain size, and the density could not be measured accurately; however, grains sink in Clerici solution (i.e., the density is greater than 4.07 g/cm^3). The calculated density is 4.69 g/cm^3. Ashburtonite is uniaxial +, $\omega = 1.786(3)$ and $\epsilon = 1.800(4)$, as determined in Na light. The lower refractive index was determined by the oil immersion method, but the immersion oils above $n = 1.785$ react with ashburtonite forming an opaque residue; thus a Berek compensator was used to determine birefringence, from which ϵ was calculated. A Gladstone-Dale calculation using the calculated density gives a compatibility index of -0.010, which is regarded as superior (Mandarino, 1981). There is no discernible fluorescence in either long- or short-wave ultraviolet light.

Ashburtonite decomposes rapidly in concentrated HCl and slowly in 0.2 *M* HCl, 1:1 HNO_3, and concentrated H_2SO_4.

Chemical composition

Chemical analysis was performed on a JEOL 733 Superprobe using Tracor-Northern 5600 automation. The wavelength-dispersive mode was used; data reduction was done with the Tracor-Northern Task series of programs using a conventional ZAF correction routine. The operating voltage was 15 kV, and the beam current was 0.020 μA. The electron beam was defocused to 20 μm and three spectrometers were used simultaneously to minimize decomposition of the sample under the electron beam. A 100-s energy-dispersive scan indicated that no elements with $Z > 9$ other than those reported here were present. Standards used were cuprite (Cu$K\alpha$), mimetite (Cl$K\alpha$), sanbornite (Si$K\alpha$), and crocoite (Pb$M\alpha$). The presence of CO_3^{2-} and OH^- ions was established by infrared spectroscopy and by crystal-structure analysis. The result of averaging analyses from four separate crystals is given in Table 1. The empirical formula based on 12 cations (Pb^{2+},Cu^{2+},Si^{4+}) is $HPb_{3.99}Cu_{4.01}Si_{4.00}O_{12.03}(HCO_3)_4(OH)_4Cl_{1.10}$. The ideal formula is $HPb_4Cu_4Si_4O_{12}(HCO_3)_4(OH)_4Cl$.

TABLE 1. Chemical composition of ashburtonite

Oxide	Wt%	Atomic proportions*		Theoretical composition (wt%) of $HPb_4Cu_4Si_4O_{12}(HCO_3)_4(OH)_4Cl$
PbO	52.17	Pb	3.99	51.44
CuO	18.66	Cu	4.01	18.33
SiO_2	14.07	Si	4.00	13.84
Cl	2.28	Cl	1.10	2.04
CO_2**	10.31	HCO_3	4.00	10.15
H_2O**	4.22	OH	4.00	4.66
	101.71	O	27.45	100.46
O = Cl	−0.51			−0.46
	101.20			100

* On basis of Pb + Cu + Si = 12.
** Calculated from stoichiometry and crystal-structure analysis. Other components determined by electron microprobe analysis.

The four analyses gave totals ranging from 100.5 to 101.8 wt%.

INFRARED ANALYSIS

High-resolution infrared spectra were recorded for the wavenumber region 400–3800 cm^{-1} using a Nicolet 5DX Fourier transform infrared spectrometer with a diamond anvil cell microsampling device. Two samples of ashburtonite approximately 1 mg in size were studied with identical results; one of the spectra is shown in Figure 3. The recorded portion between 1900 and 2400 cm^{-1} has been removed because it contains diamond spectra.

The spectrum has a large number of absorbance peaks resulting from the complex atomic structure of ashburtonite. We cannot interpret the spectrum in detail, but five bands give useful information on the gross aspects of the ashburtonite structure. The complete absence of a band near 1600 cm^{-1} indicates a lack of H_2O in the structure. The weak peak that seems to exist in that region can be attributed to adsorbed H_2O. In contrast there is a broad, intense band from 2900 to 3700 cm^{-1}, characteristic of the stretching frequency range of the OH^- ion. The broadness probably results from contributions of OH in the bicarbonate (HCO_3^-) ion in addition to regular OH^-. This is also observed for nesquehonite (Farmer, 1974). The band centered at 1350 cm^{-1} is characteristic of the asymmetric stretch, ν_3 mode, of the CO_3^{2-} group. The shift of ν_3 from approximately 1410 to 1350 cm^{-1} probably takes place because the O atoms in the CO_3^{2-} ion of ashburtonite are bonded to cations other than C, which would restrict their vibrational modes and lower the frequencies. In addition, this band is split into internal modes because of lower symmetry in the CO_3^{2-} group. The wavenumbers are 1350 and 1325 cm^{-1}. The other two bands in regions 1225–850 and 750–450 cm^{-1} are very complex, as they contain contributions from several coordination complexes, notably the SiO_4 tetrahedron and its polymerized tetrahedral ring, the Cu octahedron, and the Pb polyhedron.

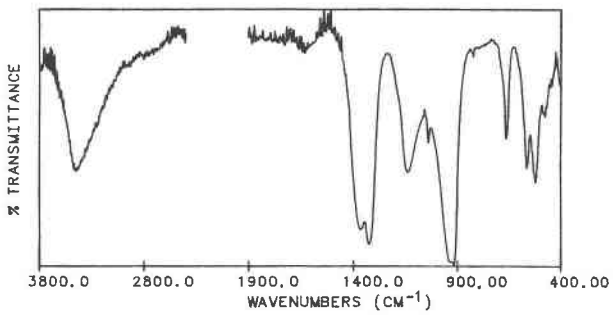

Fig. 3. Infrared spectrum of ashburtonite.

X-RAY CRYSTALLOGRAPHY AND CRYSTAL STRUCTURE DETERMINATION

Precession camera photographs show ashburtonite to be tetragonal with possible space group choices $I4/m$, $I\bar{4}$ and $I4$. As crystals of this mineral tend to be needlelike, elongate parallel to [001], c axis photograph exposures were necessarily very long, 50–70 h, using Mo radiation at 1.5 kW of power. X-ray powder-diffraction data, obtained with a Debeye-Scherrer camera having a diameter of 114.6 mm and Cu$K\alpha$ radiation, are given in Table 2.

TABLE 2. X-ray powder diffraction data for ashburtonite

hkl	d_{calc}	d_{meas}	I/I_o
110	10.065	10.2	100
200	7.117	7.14	20
101	5.609	5.644	70
220	5.033	5.039	10
310	4.501	4.495	100
400	3.558	3.583	20
321	3.315	3.333	100
420	3.183	3.192	20
411	3.005	3.013	90
202	2.804	2.805	30
222	2.609	2.611	50
312	2.526	2.522	20
440	2.516		
530	2.441	2.439	20
332	2.257	2.259	20
422	2.203	2.194	20
611	2.185		
541	2.089	2.090	20
512	2.060	2.058	10
710	2.015	2.010	30
103	2.014		
631	2.004		
640	1.974	1.971	10
213	1.938	1.935	10
532	1.906	1.910	10
730	1.869	1.866	20
721	1.862		
622	1.811	1.812	20
413	1.753	1.751	20
811	1.696	1.691	20
741	1.696		
642	1.657	1.656	30
503	1.655		
901	1.531	1.530	10
543	1.501	1.499	30
930	1.500		
921	1.497		
633	1.468	1.466	20
851	1.465		
860	1.423	1.422	10
912	1.397	1.399	10
813	1.333	1.333	20
862	1.290	1.288	30

TABLE 3. Postitional coordinates and thermal parameters (× 100, Å²) for ashburtonite

Atom	x	y	z	U_{11}	U_{22}	U_{33}	U_{23}	U_{13}	U_{12}	U_{eq}
Pb	0.21321(4)	0.03767(4)	0	1.68(4)	0.80(3)	1.51(2)	0	0	−0.01(3)	1.33(2)
Cu	¼	¼	¼	1.48(9)	1.04(8)	1.12(7)	−0.14(6)	0.22(6)	−0.74(6)	1.22(4)
Si	0.1167(3)	0.1064(3)	½	0.86(19)	0.58(19)	0.86(15)	0	0	−0.08(13)	0.77(10)
C	0.438(2)	0.859(2)	0	2.1(1.1)	6.8(1.5)	4.9(1.1)	0	0	−1.0(1.0)	4.6(7)
01	0.1637(5)	0.1455(4)	0.7245(9)	0.8(3)	0.9(3)	1.6(3)	0.4(3)	−0.4(3)	−0.6(2)	1.1(2)
02	0.3027(6)	0.1805(6)	0	0.4(5)	1.3(5)	1.3(4)	0	0	−0.1(3)	1.0(3)
03	0.0062(7)	0.1305(7)	½	0.3(5)	2.9(6)	2.6(5)	0	0	−0.1(4)	1.9(3)
04	0.3505(12)	0.8641(11)	0	6.2(1.1)	6.2(1.1)	6.7(9)	0	0	−1.1(9)	6.4(6)
05	0.4839(8)	0.8556(8)	0.1782(15)	5.7(8)	8.1(9)	10.2(9)	2.3(7)	−1.8(7)	−0.5(6)	8.0(4)
Cl	0	0	0	1.6(2)	1.6(2)	2.2(3)	0	0	0	1.8(2)

Note: Temperature factors are of the form $\exp[-2\pi^2(U_{11}h^2a^{*2} + U_{22}k^2b^{*2} + \ldots + 2U_{12}hka^*b^*)]$. Estimated standard deviations are in parentheses.

The refined unit-cell parameters are $a = 14.234(7)$ and $c = 6.103(5)$ Å with $V = 1236(1)$ Å³ and $Z = 2$.

For the intensity-data measurements, a prismatic crystal fragment measuring 0.015 × 0.04 × 0.08 mm (CMN no. 58391, xl 7) was mounted along [110]. Intensity data were collected at CANMET, Ottawa, on an Enraf Nonius CAD-4 single-crystal diffractometer operated at 52 kV and 26 mA with graphite-monochromated Mo$K\alpha$ radiation. Data measurement and reduction were done using the NRCVAX package of computer programs (Gabe et al., 1985). A set of 81 reflections permuted four ways, $\pm h$ at $\pm 2\theta$, was used to refine the cell parameters: $a = 14.1852(8)$ and $c = 6.0759(8)$ Å. A full sphere of data was obtained to $2\theta = 60°$ assuming an I-centered lattice. The intensities were corrected for Lorentz and polarization effects, and a Gaussian absorption correction ($\mu_l = 315$ cm^{-1}) was applied. The transmission factors ranged from 0.37 to 0.61. Of the 8059 measured intensities, 968 are independent, and 760 of these are observed [$F > 5.0\sigma(F)$]. It is significant that the three standard reflections decreased in intensity by 3% over the 12-days of the experiment.

The structure was solved using direct methods, and the refinement was done with the SHELXTL PC package of programs. Scattering curves for neutral atoms and anomalous dispersion corrections were taken from Cromer and Mann (1968) and Cromer and Liberman (1970), respectively. From the E map the positions of the Pb, Cu, Si, and most of the O atoms were readily determined. The difference-Fourier maps of this initial model showed additional atomic sites.

Table 3 contains the final positional and anisotropic displacement parameters; Table 4,[1] the observed and calculated structure factors; and Table 5, the selected interatomic distances and angles. The final stages of the least-squares refinement involved a conversion to anisotropic temperature factors and the addition of a weighting scheme of $[\sigma^2(F)]^{-1}$. This resulted in final residual indices of $R = 3.5\%$ and $R_w = 2.4\%$ using 762 observed reflections to refine the 65 least-squares parameters. An extinction correction was tried, but it did not improve the refinement.

Each of the possible space groups was refined using all the intensity data and the weighting scheme prescribed by Hamilton (1965). The Rg for each of the space groups $I4/m$, $I4$, and $I\bar{4}$ are 2.61, 2.51, and 2.45, respectively. Using Hamilton's (1965) R-factor ratio test, the statistics indicate a slight preference for the $I\bar{4}$ space group but this

[1] A copy of Table 4 may be ordered as Document AM-91-469 from the Business Office, Mineralogical Society of America, 1130 Seventeenth Street NW, Suite 330, Washington, DC 20036, U.S.A. Please remit $5.00 in advance for the microfiche.

TABLE 5. Selected interatomic distances (Å) and angles (°) in ashburtonite

	Si tetrahedron			**C triangle**	
Si-01	1.616(6) ×2		C-04	1.24(3)	
Si-03	1.605(10)		C-05	1.27(2) ×2	
Si-03	1.609(10)		Mean	1.26	
Mean	1.611		04-05	2.18(2)	121(1) ×2
01-03	2.63(1)	109.3(3) ×2	05-05	2.16(2)	117(2)
01-03	2.59(1)	106.9(3) ×2			
01-01	2.73(1)	115.1(5)		**Cu octahedron**	
03-03	2.62(1)	109.3(8)	Cu-01	1.929(6) × 2	
			Cu-02	1.959(6) × 2	
	Pb polyhedron		Cu-04	2.638(13) × 2	
Pb-01	2.374(6) ×2		01-02	2.63(1)	94.7(3) ×2
Pb-02	2.391(9)		01.02	2.86(1)	85.3(3) ×2
Pb-03	3.315(4) ×2		01-04	3.15(1)	94.1(4) ×2
Pb-04	3.139(16)		01-04	3.15(1)	85.9(4) ×2
Pb-05	2.829(11) ×2		02-04	3.19(1)	86.6(3) ×2
Pb-C1	3.071(1)		02-04	3.19(1)	93.4(3) ×2

Note: Estimated standard deviations are in parentheses.

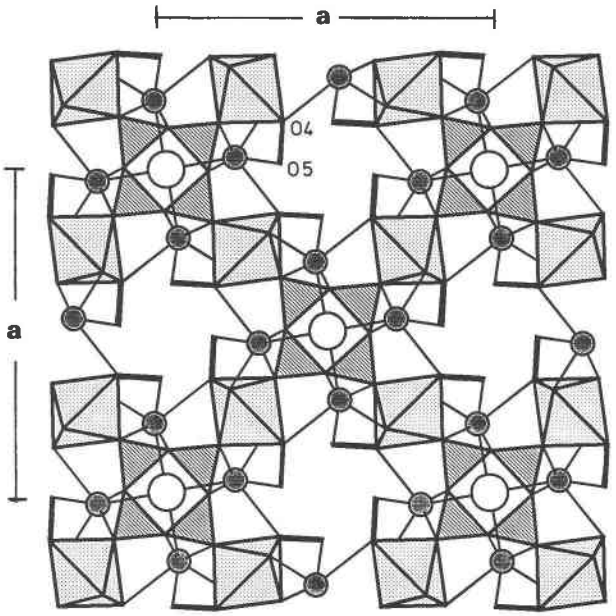

Fig. 4. A **c** axis projection of the ashburtonite structure showing four-membered Si tetrahedral rings and (stippled) Cu octahedra. Pb atoms are filled circles, Cl atoms are open circles, and CO_3 groups are shaded triangles with planes approximately parallel to (100).

result cannot be considered significantly better than that of $I4/m$ in view of the large systematic errors involved in the absorption correction of the intensity data. The dipyramidal morphology of some crystals indicates point group $4/m$, which suggests that the preferred space group should be $I4/m$. All of the structure results tabulated in this paper will therefore be for space group $I4/m$, but the structure model for space group $I\bar{4}$ has some appealing aspects that will be discussed later.

Description and discussion of the structure

The basic structural motif of the ashburtonite structure is a four-membered, tetrahedral silicate ring (Fig. 4). Very few minerals have this type of ring structure. Liebau (1985) lists six minerals (papagoite, kainosite, joaquinite, taramellite, baotite, and nagashimalite) and three synthetic phases [$HKSi_3O_{12}$, $K_2ScSi_2O_6(OH)$, and Pb_2SiO_4]. Finger et al. (1989) recently described another synthetic phase and noted that in $BaCuSi_2O_6$ the four-membered ring has point symmetry $2mm$, which is higher symmetry than any so far reported for structures of this class. In ashburtonite, the silicate ring has point symmetry $4mm$ that seems to dominate the overall topology of the structure.

The [SiO_4] tetrahedra are cross linked by octahedrally coordinated Cu. The Jahn-Teller distortion in the Cu octahedron is very evident, with Cu-O bond lengths of 2.62 Å along the apices, and pairs of 1.93 and 1.96 Å bond lengths in the equatorial plane. The Cu octahedra form edge-sharing ribbons parallel to the c axis (Fig. 5).

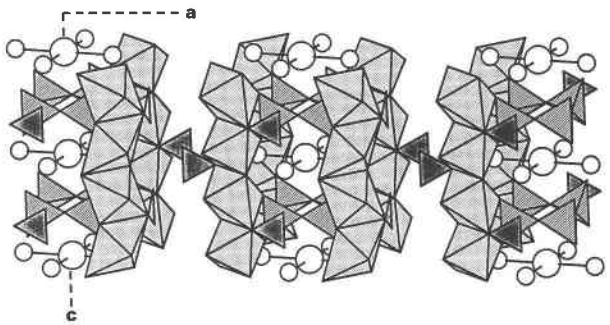

Fig. 5. An inclined **a** axis projection of the ashburtonite structure showing ribbons of Cu octahedra, four-membered Si tetrahedral rings, and CO_3 groups in the **c** axis channels. Pb atoms are small open circles, and Cl atoms are larger open circles.

Pb plays a major role in this structure by bonding to all the major polyhedra, Si, Cu, and C. Figure 6 shows this odd, large Pb^{2+} coordinate complex, which has five regular Pb-O bond lengths varying from 2.38 to 2.84 Å on one side of the polyhedron and three longer Pb-O bonds (3.14–3.31 Å) and a Pb-Cl bond (3.07 Å) on the other side. Probably the long-bonded portion of the polyhedron has a lone pair of electrons that spread out these bonds. In fact, the stereochemically inactive lone-pair electrons of Pb effect a major shift in the Pb position and destroy the mirror planes of point symmetry $4mm$ established by the four-membered tetrahedral ring of Si. This displacement of Pb^{2+} from higher symmetry sites has been noted in hyalotekite (Moore et al., 1982), joesmithite (Moore, 1988), and beudantite (Szymański, 1988).

Liebau (1985) points out the importance of the presence of highly electronegative cations such as Pb and Cu, which inhibit silicate chain formation in favor of a tight ring complex. These cations effectively reduce the electrostatic repulsive forces between adjacent SiO_4 tetrahedra, thus stabilizing the ring formation. Common elements that would inhibit this structure type are Mg, Mn,

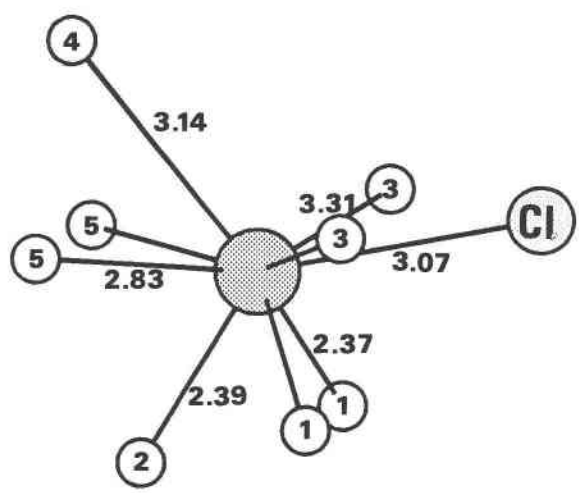

Fig. 6. Pb polyhedron in ashburtonite structure.

and Fe, all notably minor in concentration in the ashburtonite assemblage and completely absent in ashburtonite itself.

The Cl^- ion lies on the tetrad axis midway between silicate rings (Fig. 5). It is located at the center of a square plane of four Pb atoms similar to that in the taramellite structure (Mazzi and Rossi, 1980). Similar to Pb and Cu, the highly electronegative atom Cl effectively stabilizes the four-membered silicate ring by reducing the average negative charge on each SiO_4 tetrahedron (i.e., an electron sink).

Although the number and location of H atoms could not be determined from Fourier synthesis, bond-valence calculations for each O site, based on the constants of Brown (1981), helped delineate their distribution. The bond-valence sums for the O atoms are O1 2.04, O2 1.32, O3 2.26, O4 1.95, and O5 1.58 vu. This leads us to conclude that O2 is an OH anion and that O5 has an H atom shared in part between two symmetry related O atoms bonded to C, making a bicarbonate group $[HCO_3]^-$. If the space group is lowered in symmetry to $I\bar{4}$, these two O atoms are no longer symmetry related by the mirror plane, and the bond-valence sum is markedly lower for one of them, 0.91 vs. 1.70 vu. This is the one feature that favors the $I\bar{4}$ model as mentioned previously. Based on the above information, the simplest chemical formula is $Pb_4Cu_4Si_4O_{12}(HCO_3)_4(OH)_4Cl$, but this formula needs one additional positive charge for charge balance. From bond-valence calculations, it appears that Pb (1.99 vu) and Cu (2.07 vu) are nearly saturated. It is quite possible that the "missing" positive charge is a proton in the channels associated with the bicarbonate group as a hybrid of $[HCO_3]^-$ and $[H_2CO_3]$. There are reasons for proposing this interesting hybrid. Both O4 and O5 have large displacements on the order of those expected for OH, and both of these O atoms have low bond-valence sums. In the $I\bar{4}$ model all three bicarbonate O atoms have similar characteristics. The H ions probably do not always bond to the same O atom, but one or two could be shared at each bicarbonate group.

In Figure 4 the trigonal plane of $[CO_3]$ in the bicarbonate group is not evident as it is approximately parallel to (100) and hence appears as a line in this projection. Yet Figure 4 does show clearly how large this channel is, and although the CO_3 anion is anchored through 04 to the Cu octahedron on one end, the other ends are only loosely bonded to Pb through two O5 atoms. The large thermal displacement factors for the atoms involved (C, O4, and O5) show how loosely bonded it is. The bond distance of O5-O5 of 2.63 Å across this open channel is good evidence for H bonding between bicarbonate groups. This has been noted in the crystal structures of nahcolite (Zachariasen, 1933) and teschemacherite (Brooks and Alcock, 1950) where H-bonded bicarbonate groups form chains. Two carbonate anions share one H (Pertlik, 1986) in trona.

Very few minerals are described as bicarbonates, and only a small portion of these have had their crystal structures determined. Within the earth's weathering profile there are wide Eh and pH ranges compatible with the formation of bicarbonates; perhaps their apparent rarity in numbers of species is only because the techniques commonly used to analyze minerals do not differentiate this chemical class. A good crystal structure analysis is required to recognize a bicarbonate, and this paper further supports this method as a valid and useful chemical analytical technique (Hawthorne and Grice, 1990). Some of the details of proton distribution could be resolved with neutron diffraction studies, but the small crystal size precludes this type of experiment at present.

Acknowledgments

The authors are grateful to the following for their cooperation and support in this project: J.T. Szymański, Canada Centre for Mineral and Energy Technology, Ottawa, for permission to use the single-crystal diffractometer; Y. Lepage, National Research Council of Canada, Ottawa, for providing computer facilities; R.S. Williams, Canadian Conservation Institute, Ottawa, for the infrared analysis; B.W. Robinson, Commonwealth Scientific and Industrial Research Organization, Perth, for electron-microprobe analysis; T.S. Ercit, Canadian Museum of Nature, for assistance with the electron microprobe analysis; and R. Dinn, Canadian Museum of Nature, Ottawa, for typing the manuscript. The reviews of L.W. Finger and F.F. Foit, Jr. greatly improved this manuscript.

References cited

Brooks, R., and Alcock, F.C. (1950) Crystal structure of ammonium bicarbonate and a possible relationship with ammonium hypophosphate. Nature, 166, 435–436.

Brown, I.D. (1981) The bond-valence method: An empirical approach to chemical structure and bonding. In M. O'Keefe and A. Navrosky, Eds., Structure and bonding in crystals, p. 1–30. Academic Press, New York.

Cromer, D.T., and Liberman, D. (1970) Relativistic calculation of anomalous scattering factors for X-rays. Journal of Chemical Physics, 53, 1891–1898.

Cromer, D.T., and Mann, J.B. (1968) X-ray scattering factors computed from numerical Hartree-Fock wave functions. Acta Crystallographica, A24, 321–324.

Farmer, V.C. (1974) The infrared spectra of minerals. Mineralogical Society Monograph 4, 539 p. Mineralogical Society, London.

Finger, L.W., Hazen, R.M., and Hemley, R.J. (1989) $BaCuSi_2O_6$: A new cyclosilicate with four-membered tetrahedral rings. American Mineralogist, 74, 952–955.

Gabe, E.J., Lee, F.L., and Lepage, Y. (1985) The NRCVAX crystal structure system. In G.M. Sheldrick, C. Kruger, and R. Goddard, Eds., Crystallographic computing 3: Data collection, structure determination, proteins and data bases, p. 167–174. Clarendon Press, Oxford.

Hamilton, W.C. (1965) Significance tests of the crystallographic *R* factor. Acta Crystallographica, 18, 502–510.

Hawthorne, F.C., and Grice, J.D. (1990) Crystal structure analysis as a chemical analytical method: Application to first-row elements. Canadian Mineralogist, 28, 693–702.

Liebau, F. (1985) Structural chemistry of silicates, 347 p. Springer-Verlag, Berlin.

Mandarino, J.A. (1981) The Gladstone-Dale relationship: Part IV. The compatibility concept and its application. Canadian Mineralogist, 19, 441–450.

Mazzi, F., and Rossi, G. (1980) The crystal structure of taramellite. American Mineralogist, 65, 123–128.

Moore, P.B. (1988) The joesmithite enigma: Note on the 6s $^2Pb^{2+}$ lone pair. American Mineralogist, 73, 843–844.

Moore, P.B., Araki, T., and Ghose, S. (1982) Hyalotekite, a complex lead borosilicate: Its crystal structure and the lone-pair effect of Pb(II). American Mineralogist, 67, 1012–1020.

Nickel, E.H., Robinson, B.W., Fitzgerald, J., and Birch, W.D. (1989) Gar-

trellite, a new secondary arsenate mineral from Ashburton Downs, W.A. and Broken Hill, N.S.W. Australian Mineralogist, 4, 83–89.

Pertlik, F. (1986) Ein Vergleich von Ergebnissen routinemäßiger Strukturbestimmungen mittels Röntgen—BZW. Neutronen-Einkristalldaten am Beispiel der Trona, $N_3H[CO_3]_2 \cdot 2H_2O$. Mitteilungen der Osterreichischen Mineralogischen Gesellschaft, 131, 7–13.

Szymański, J.T. (1988) The crystal structure of beudantite, $Pb(Fe,Al)_3[(As,S)O_4]_2(OH)_6$. Canadian Mineralogist, 26, 923–932.

Zachariasen, W.H. (1933) The crystal lattice of sodium bicarbonate, $NaHCO_3$. Journal of Chemical Physics, 1, 634–639.

Manuscript received November 9, 1990
Manuscript accepted May 21, 1991